Computers and Concrete, *Vol. 36, No. 4 (2025) 445-453*
https://doi.org/10.12989/cac.2025.36.4.445

Mechanical, shrinkage and chloride ion erosion resistance of concrete prepared with recycled aggregates by heating

Xiaohui Yan, Ting Liu*, Bei Zhang and Hongmei Wang

Department of Municipal and Ecological Engineering, Shanghai Urban Construction Vocational College, Shanghai 200438, China

(*Received December 9, 2024, Revised December 12, 2024, Accepted May 27, 2025*)

Abstract. This study explored the effects of recycled aggregates (RA) by modifying the shrinkage and chloride penetration resistance of concrete. RA was heated at constant temperatures of 300, 500, and 700 ℃ for 30 min. Further, the measured shrinkage and chloride penetration resistance of the recycled aggregate concrete (RAC) were also adversely affected by the incorporation of RA. The results indicated that replacing 50% of NA with RA reduced compressive strength by 28.5% at 28 days. Shrinkage values for 100% RA replacement increased by 65.7% at 28 days compared to the reference, while chloride ion penetration (electric flux) doubled. Moreover, when the heating temperature of RA was lower than 500 ℃, the compressive strength of RAC increased with increasing temperature and decreased when the temperature exceeded 500 ℃. The shrinkage value and chloride ion penetration resistance of the RAC exhibited similar phenomena. The addition of secondary cementitious materials contributed to the compressive strength, shrinkage, and chloride penetration resistance of RAC. Heating RA at 500 ℃ improved compressive strength by 12.3% compared to untreated RA, reduced porosity to 15.3%, and minimized shrinkage. Incorporating 20% fly ash (FA) and 10% granulated blast-furnace slag (GBFS) enhanced compressive strength by 9.6% and reduced chloride flux by 27% at 120 days. In addition, pore structure characteristics were investigated, and it was found that the pore structure of RAC also improved owing to the heating of RA.

Keywords: chloride penetration; heating modification; pore structure; recycled aggregates; shrinkage

1. Introduction

Over the past several decades, the global construction sector has experienced significant growth, particularly in emerging economies. This surge in construction has led to substantial consumption of materials, creation of substantial construction and demolition debris, and environmental degradation. Given that concrete is a primary material in construction, enhancing the sustainability of the industry can be achieved by reducing the environmental footprint of concrete. Presently, utilizing construction and demolition waste to produce recycled materials, such as recycled concrete, has become a prevalent strategy in many nations to promote the recycling of construction and demolition materials (Behzad *et al.* 2019, Lotfi *et al.* 2015, Wang *et al.* 2017). The construction industry converts by-products (steel slag and recycled concrete) into high-performance structural concrete via low-cost methods, with large-scale tests confirming good workability, strength, and durability, despite minor issues like higher density, plastic shrinkage, and reduced chloride resistance, proving viable for most structural applications (Amaia *et al.* 2023). Ledesma (Ledesma *et al.* 2016) has evaluated the feasibility of replacing natural sand with recycled concrete sand, adjusting water for consistency, and analyzing fresh/hardened properties to determine statistically significant impacts of replacement levels on performance.

Recycled aggregates (RA) are primarily derived from the crushing and processing of waste materials generated from construction and demolition activities. These RA are employed to substitute natural aggregates (NA), either partially or entirely, in the production of recycled aggregate concrete (RAC). The composition of RAC is notably more intricate than that of concrete made with natural aggregates. This complexity arises from the presence of three distinct types of interfacial transition zones (ITZ) within the RAC. These zones are formed by the adherence of old mortar to the RA, which includes the interface between RA and old mortar, between RA and new mortar, and between old mortar and new mortar (Zhang *et al.* 2015). These interfaces impact the mechanical properties, shrinkage behavior, and resistance to chloride ion penetration of the RAC (Jiong *et al.* 2015, Tran M. *et al.* 2023, Xiao *et al.* 2015). Research (Pedro *et al.* 2014, Seara-Paz *et al.* 2018, Xiao *et al.* 2015, Zega *et al.* 2015) has consistently indicated that concrete mixtures incorporating RA typically exhibit lower compressive strengths compared to those made with NA. Moreover, as the proportion of RA replacement increases, so does the amount of old mortar, which in turn diminishes the mechanical performance of the RAC. Seara-Paz *et al.* (2016) has investigated the mechanical properties (compressive strength, tensile splitting strength, modulus of elasticity) of structural concrete with varying recycled coarse aggregate (RCA) replacement ratios (0%, 20%, 50%, 100%) and water-to-cement ratios (0.50, 0.65), revealing that mechanical behavior depends on RCA replacement levels and inherent

*Corresponding author, Professor
E-mail: 406779136@163.com

ISSN: 1598-8198 (Print), 1598-818X (Online)

aggregate characteristics. Xiangyi *et al.* (2018) research using experiments and PFC3D simulations showed that increasing recycled aggregate content reduces the compressive, tensile, and flexural strengths of pervious concrete. Fiol *et al.* (2023) has validates industrial-scale use of self-compacting concrete (SCC) with 100% coarse recycled aggregate (RA) in precast applications, demonstrating failure loads 1.5-3 times above requirements, comparable elastic behavior to RA-free SCC. Sainz-Aja *et al.* (2022) investigates the fatigue behavior of recycled aggregate concrete (RAC) under moderate (10 Hz) and high-frequency (90 Hz) loading, revealing that high-frequency tests significantly reduce the fatigue limit, with specimen temperatures reaching 100 ℃ under overload conditions, inducing pronounced creep damage (particularly in RAC), thereby demonstrating the synergistic degradation mechanism of elevated temperature and high-frequency loading, offering critical insights for optimizing fatigue testing protocols in recycled concrete applications.

Shrinkage characteristics are also a critical aspect of concrete. The majority of empirical studies have demonstrated a direct correlation between the shrinkage of RAC and the proportion of RA used (Domingo *et al.* 2009, Seara-Paz *et al.* 2016, Zhang *et al.* 2020,). However, there are exceptions where the findings contradict this trend. For instance, Soberón (2002) observed a decrease in the shrinkage rate of RAC with an increase in the RA replacement ratio. The study further revealed that the shrinkage resistance of RAC prepared from RA is influenced by the strength of the original concrete from which the RA is derived. The stronger the parent concrete, the better the shrinkage resistance of the resulting RAC (Gholampour *et al.* 2018). Additionally, it has been noted that RAC generally exhibits inferior durability compared to conventional concrete. This is evident in aspects such as the RAC's resistance to chloride ion penetration (Sasanipour *et al.* 2019) and other related durability issues (Abdelaziz *et al.* 2022, Comingstarful *et al.* 2018, Mahdi *et al.* 2019, Pedro *et al.* 2017). Besides, Fiol *et al.* (2023) has studied the durability of self-compacting concrete (SCC) with varying coarse recycled precast-concrete aggregate (RPCA) and cement contents in marine environments, showing that increased cement content mitigates RPCA-induced porosity (25% reduction in effective porosity from 28 to 180 days), improves water absorption and carbonation resistance.

In summary, the above studies show that the existence of the old mortar would have varying degrees of effect on the compressive strength, shrinkage and chloride penetration resistance of RAC. Some researchers have carried out a series of studies on how to improve the properties of RA. Some of the techniques were removing or strengthening of the adhered mortar (Grabiec *et al.* 2012, Kong *et al.* 2010, Pelisser *et al.* 2011, Su *et al.* 2015), two or triple stage mixing method (Kong.2010, Rajhans.2019, Rajhans.2018), and addition of supplementary cementitious materials such as fly ash (FA), granulated blast-furnace slag (GBFS), silica fume etc. to the RAC (Ya *et al.* 2021, Kou *et al.* 2011, Kou *et al.* 2013). However, the results showed that although these technologies have certain positive effects, they cannot eliminate the influence of the old mortar on RAC. Additionally, nanomaterials could also improve the properties of RAC, and the results were satisfactory. However, the high price of nanomaterials and their dispersion limited the use in RAC (Ji *et al.* 2005, Mukharjee *et al.* 2014). The carbonization treatment of RA was an effective and environmentally friendly method to improve the performance of RAC (Shi *et al.* 2016, Xiang *et al.* 2023). However, this technology was complicated and required specific equipment.

In this paper, the recycled aggregate was modified by heating to study the durability of the recycled concrete. Since, the mechanical property is the vital property of concrete, the compressive strength of RAC was first investigated in this paper. Further, the shrinkage and chloride penetration resistance of RAC were evaluated. In addition, the pore characteristics were also discussed.

Table 1 Physical properties of cement

Compression Strength (MPa)		Flexural Strength (MPa)		Setting Time (min)		Specific Surface Area (m^2/kg)
3 d	28 d	3 d	28 d	Initial	Final	
18.7	46.3	3.6	7.1	252	301	348

Table 2 Properties of aggregates

Aggregates Type	Apparent Density (kg/m^3)	Water Absorption (%)	Crushing Index (%)
Coarse NA	2725	0.46	6.3
Coarse RA	2560	2.32	9.6
Fine NA	2645	1.11	7.4
Fine RA	2535	4.57	14.7

2. Materials and experiment

2.1 Materials

2.1.1 Cement

P.O.42.5 ordinary cement was used in this test. Physical properties of cement are presented in Table 1.

2.1.2 Aggregates

The coarse NA with a particle size of 5mm~25mm were used. The fine NA used in the test was medium sand. The main properties of coarse NA and fine NA were measured according to the Chinese Standard JGJ52-2006, and the results are shown in Table 2. RA included fine RA and coarse RA. The recycled aggregate was heated at 300 ℃, 500 ℃ and 700 ℃ for a constant temperature of 30 min, marked RA-300, RA-500 and RA-700, respectively, and then put into the concrete shaking table for vibration time of 15 min (Su *et al.* 2015). The main properties of fine RA and coarse RA were measured according to the Chinese Standards GB/T25176-2010 and GB/T 25177-2010, respectively, and the results are shown in Table 2.

2.1.3 Secondary cementitious materials

The secondary cementitious materials included FA and GBFS. The FA used in this paper was grade Ⅱ fly ash, with a

Table 3 Mix proportions of concrete

No.	Coarse RA Type	Coarse RA Replacement Percentage (%)	W/C	Design of Mix Proportion (kg/m^3)						
				Cement	Coarse NA	Coarse RA	Fine NA	FA	GBFS	SP
A-0	NA	0		450	1010	-		-	-	
A-1	RA-500	20		450	808	202		-	-	
A-2	RA-500	40		450	606	404		-	-	
A-3	RA-500	50		450	505	505		-	-	
A-4	RA-500	100		450	-	1010		-	-	
B-1	RA-300	20	0.35	450	808	202	975	-	-	5.4
B-2	RA-500	20		450	808	202		-	-	
B-3	RA-700	20		450	808	202		-	-	
C-1	RA-500	20		360	808	202		90	-	
C-2	RA-500	20		405	808	202		-	45	
C-3	RA-500	20		315	808	202		90	45	

Table 4 Mix proportions of mortar

No.	Fine RA Type	Fine RA Replacement Percentage (%)	W/C	Design of Mix Proportion (kg/m^3)					
				Cement	Fine NA	Fine RA	FA	GBFS	SP
D-0	NA	0		525	1500	-	-	-	
D-1	RA-500	20		525	1200	300	-	-	
D-2	RA-500	40		525	900	600	-	-	
D-3	RA-500	50		525	750	750	-	-	
D-4	RA-500	100		525	-	1500	-	-	
E-1	RA-300	20	0.35	525	1200	300	-	-	5.4
E-2	RA-500	20		525	1200	300	-	-	
E-3	RA-700	20		525	1200	300	-	-	
F-1	RA-500	20		420	1200	300	105	-	
F-2	RA-500	20		427.5	1200	300	-	52.5	
F-3	RA-500	20		367.5	1200	300	105	45	

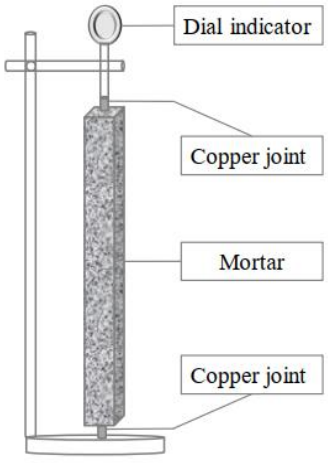

Fig.1 The specimen shrinkage test

specific surface area of 443 m^2/kg and a density of 2470 kg/m^3. The GBFS used in this paper was S95 grade powder with a specific surface area of 415 m^2/kg and a density of 2860 kg/m^3.

2.1.4 Additives

A polycarboxylate superplasticizer (SP) was used as an admixture in 1.2% proportions of cement mass.

2.2 Mix proportions

The mix proportions of the concrete and mortar are provided in Tables 3 and 4, respectively. According to the specifications mentioned in section 2.3, out of all these specimens, the concrete specimens were used for strength and chloride penetration tests, and the mortar specimens were used for shrinkage test. The specimens for each test were divided into three groups. No. A-0 and No. D-0 were used as the reference specimens.

2.3 Test methods

2.3.1 The strength of RAC

The compressive and tensile strengths of RAC were determined on the 100×100×100 mm cube specimens according to Chinese Standard JTGE30-2005. The compressive and tensile strengths of the hardened RAC

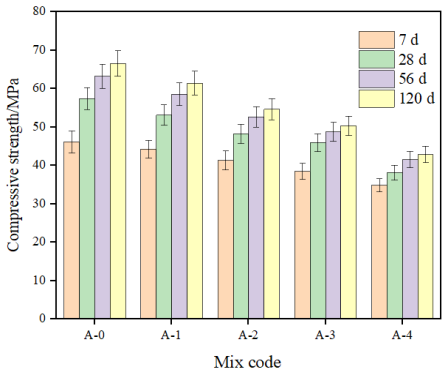

(a) Effect of the RA replacement percentage

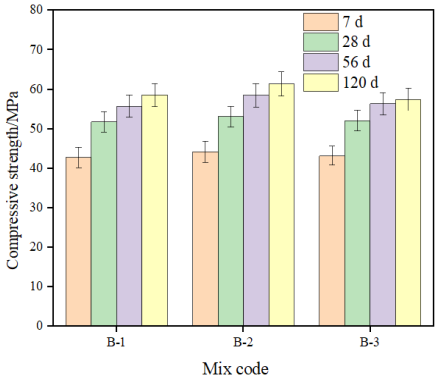

(b) Effect of the RA heating temperature

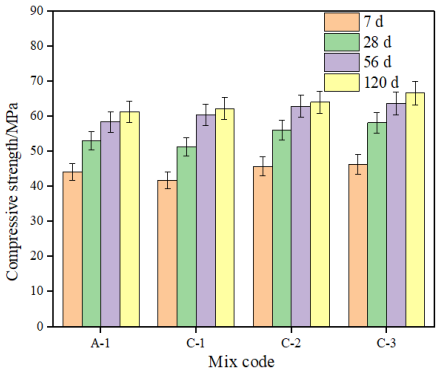

(c) Effect of the secondary cementitious materials

Fig. 2 The compressive strength of RAC

were determined at the ages of 7, 28, 56 and 120 days.

2.3.2 Shrinkage of mortar

The drying shrinkage of mortar was tested by measuring the specimens length change in accordance with Chinese standard JCT603-2004. The mortar specimens were prism of size 25×25×280 mm. Each specimen was fitted with a copper joint at both ends. The specimens were taken out from the molds 1 d after casting and the length of the specimens were measured immediately. Then the specimens were placed under the conditions of 20±3 ℃ and the relative humidity of 50%±4%. The specimen shrinkage test is shown in Fig. 1 and the formula of the shrinkage of the mortar is given in Eq. (1).

$$\xi_t = \frac{L_0 - L_t}{L - L_d} \tag{1}$$

where ξ_t is the shrinkage value of the specimen at t d (%), L_0 is the initial length of the specimen (mm), which is the value measured at 1 d, L is the length of the specimen (mm), which is 280 mm, L_d is the total length of the two copper joints inserted in the mortar, which is 20±2 mm, and L_t is the measured length of the specimen at t d (mm).

2.3.3 Chloride penetration

The chloride ions penetration of concrete was proceeded using the coulomb electric flux method conforming to Chinese Standard GB/T50082-2009.The size of the concrete specimen was a cylindrical specimen with a diameter of 100±1mm and a height of 50±2mm. According to the Chinese Standard GB/T50082-2009, the electric flux of the specimen can be approximated by Eqs. (2) and (3).

$$Q_{100} = 900(I_0 + 2I_{30} + 2I_{60} + \cdots + 2I_t \ldots + 2I_{300} + 2I_{330} + I_{360}) \tag{2}$$

$$Q_g = Q_{100} \times (95/100)^2 \tag{3}$$

where Q_{100} is the electric flux of the specimen with diameter 100 mm (C), I_0 is the initial current (A), I_t is the current at time t min (A), Q_g is the electric flux of the specimen with diameter 95 mm (C).

2.3.4 Pore structure test

A cutting machine was used to cut the recycled concrete specimen into a size of about 15 mm×15 mm×15 mm for testing. The test was carried out with the MicroActive AutoPore V 9620 high performance fully automatic mercury injection instrument with a contact Angle of 130.000 ° and pressure from 0.10 to 61000.00 psia step by step. The pore structure characteristics of recycled concrete were analyzed by the volume number of mercury injected under low pressure and high pressure.

3. Results and discussion

3.1 The compressive strength of RAC

Fig. 2(a) illustrates the experimental outcomes regarding how the proportion of recycled aggregates (RA) influences the compressive strength of recycled aggregate concrete

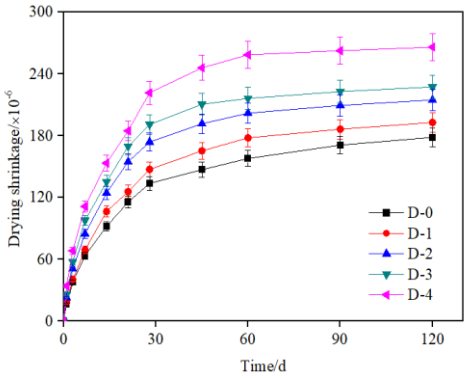

(a) Effect of the RA replacement percentage

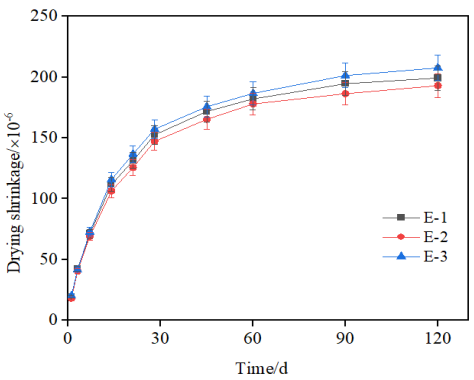

(b) Effect of the RA heating temperature

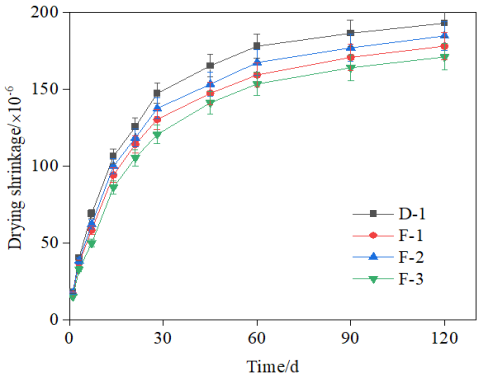

(c) Effect of the secondary cementitious materials

Fig. 3 The shrinkage of recycled mortar

(RAC). It is evident that the compressive strength of RAC generally rises with the extension of the curing period. Moreover, it is observed that an increase in the RA replacement ratio correlates with a decrease in the compressive strength of RAC at different ages, with both being consistently lower than that of the reference concrete. The incorporation of RA leads to an uneven distribution of strength within the skeletal materials of RAC (Zhang *et al.* 2015). Furthermore, the presence of internal micro-cracks, elevated porosity, and enhanced water absorption in RA contribute to the reduced mechanical properties of RAC when compared to the reference concrete.

Fig. 2(b) shows the test results of the influence of RA heating temperature on the compressive strength of RAC. It can be seen from Fig. 2(b) that the compressive strength of B-1 and B-2 increases with the increase of RA heating temperature. With the increase of RA heating temperature, the intensity of RAC has a tendency to decrease. This may be due to the fact that when the heating temperature rises to 300℃, the old mortar structure carried by the recycled aggregate becomes loose, and part of the mortar on the aggregate surface falls off through the action of the concrete shaking table, the aggregate performance index was improved compared with that without modification. When the heating temperature was 500 ℃, due to the thermal expansion of aggregate and mortar, the mortar structure was further damaged, and the mortar and aggregate fall off as a whole at the interface, and the performance of regenerated coarse aggregate basically reaches the performance of its internal coarse aggregate.When the heating temperature was 700 ℃, the regenerated coarse aggregate may have been partially damaged by high temperature, which ultimately leads to the deterioration of the mechanical properties of RAC.

Fig. 2(c) delineates the impact of secondary cementitious materials on the mechanical properties of recycled aggregate concrete (RAC). At 28 d, C-1 exhibited a 3.2% decrease in compressive strength relative to A-1, while C-2 and C-3 recorded increases of 5.6% and 9.6%, respectively. By 120 d, C-1, C-2, and C-3 saw further increases in compressive strength by 1.5%, 4.5%, and 8.6%, respectively. Corinaldesi *et al.* (2020) has demonstrated that high-volume fly ash (HVFA) recycled aggregate concrete achieves comparable mechanical properties, reduces carbonation and chloride penetration.The initial low reactivity of FA resulted in a decelerated strength gain in RAC, yet its pozzolanic properties significantly contributed to strength enhancement at later stages. The pozzolanic reactions refined RAC's internal pore structure (Kou *et al.* 2013), augmenting its density and strength. GBFS with its smaller particle size and higher activity (Kapoor *et al.* 2016), facilitated early strength development in RAC. The incorporation of FA and GBFS promoted a more comprehensive secondary hydration process, leading to an increased formation of C-S-H gel, which in turn, elevated the density and strength of RAC (Kou *et al.* 2013).

3.2 The shrinkage of mortar

Figs. 3(a)-(c) are the test results of the shrinkage of

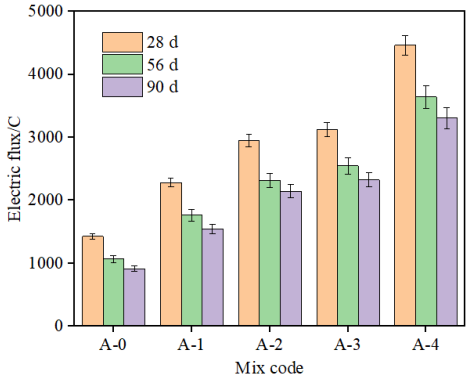

(a) Effect of the RA replacement percentage

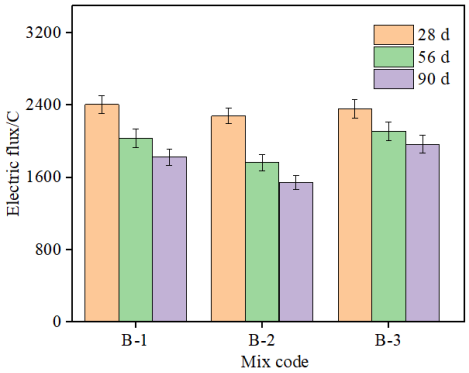

(b) Effect of the RA heating temperature

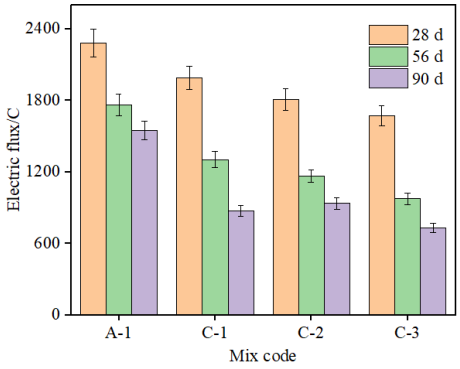

(c) Effect of the secondary cementitious materials

Fig. 4 The coulomb electric flux of concrete

recycled mortar on the three factors of RA replacement percentage, RA heating temperature and secondary cementitious materials. The following conclusions can be drawn from Fig. 3.

(1) Fig. 3(a) indicates that the shrinkage values of recycled mortar exceeded those of the reference mortar, with an increase in shrinkage as the substitution rate of fine RA rose. Initially, the shrinkage values of RAC with varying RA replacement percentages were relatively similar, possibly because the fine RA absorbed moisture during mixing, providing an internal curing effect that mitigated shrinkage from early moisture loss. The Fig. 3(a) also illustrates that shrinkage values increased rapidly at the beginning and then decelerated over time. At 28 d, the shrinkage values for D-1, D-2, D-3, and D-4 were 10.1%, 30.0%, 42.7%, and 65.7% higher than D-0, respectively. At 120 d, the corresponding increases were 8.1%, 20.3%, 27.5%, and 49.1%. The porosity of RA, especially in highly porous recycled mortar, significantly influenced the extent of shrinkage increase. When a humidity gradient was present between the recycled mortar and the surrounding environment, increased RA porosity led to greater moisture loss from the cement paste. Additionally, the inclusion of RA decreased the Young's modulus of the recycled mortar, contributing to increased shrinkage (Butler *et al.* 2013, Dapena *et al.* 2011).

(2) Fig. 3(b) shows that when RA heating temperature was 500 ℃, the shrinkage rate of recycled mortar changes the least. The possible reason was that as the temperature rises, the old mortar carried by the recycled aggregate was peeled off, which made the performance of the recycled aggregate enhanced, but when the temperature exceeds 700 degrees, the recycled aggregate was damaged, so that the shrinkage performance of the recycled concrete was reduced.

(3) Shrinkage values for F-1, F-2, and F-3 were all observed to be lower than those for D-1, with F-3 showing the greatest reduction, followed by F-1, and F-2 the least. This reduction is attributed to the substitution of a portion of the cement with secondary cementitious materials, effectively decreasing the volume of hydration products. The secondary reaction of FA and GBFS with cement hydration products forms additional gels that fill the pores in the recycled mortar, enhancing its compactness and impeding the diffusion and evaporation of moisture, thus curtailing drying shrinkage. FA, characterized by its spherical microbeads and dense texture, offers a superior filling effect in the microstructure of recycled mortar compared to the amorphous GBFS particles. Consequently, mortar containing FA experiences reduced drying shrinkage compared to that with GBFS. The addition of FA and GBFS optimizes the particle size distribution of the cementitious materials, leading to a coordinated reduction in shrinkage performance.

3.3 The coulomb electric flux of RAC

Fig. 4(a) illustrates the impact of RA replacement ratios on the electric flux of RAC. The electric flux of RAC at all ages was noted to exceed that of the reference concrete,

Table 5 Pore structure characteristics of RAC

Temperature (℃)	Porosit (%)	Total Pore Volume (mL/g)	Total Pore Area (m^2/g)	Average Pore Size (nm)
300	18.124	0.0907	6.721	61.32
500	15.347	0.0814	6.064	48.14
700	17.335	0.0871	6.827	60.53

with an increase in RA replacement leading to a proportional rise in electric flux. Over time, the electric flux of the concrete decreases. Specifically, at 28 days, the electric flux of RAC with a 50% RA replacement was 1.19 times higher than the reference concrete, and for 100% RA replacement, it was 2.12 times higher. The increase in RA replacement percentage correlates with a rise in the number of interfacial transition zones, which in turn amplifies the pathways for chloride ion penetration, diminishing the chloride ion resistance of RAC. Bravo's research (Bravo *et al.* 2015) indicates that an increase in the old mortar adhering to RA, indicative of higher porosity and more interfacial transition zones, results in a reduced ability of RAC to resist chloride penetration. Consequently, a higher RA replacement percentage equates to a poorer resistance to chloride ion penetration in RAC.

Fig. 4(b) shows the influence of the heating temperature of RA on the electric flux of RAC. The results of Fig. 4(b) show that after 500℃, the electric flux of RAC increased slightly with the increase of temperature. It may be due to the high temperature damage of RA, which led to the increase of micro cracks in RAC, and reduced the resistance of RAC to chloride ion penetration.

Fig. 4(c) delineates the influence of secondary cementitious materials on the electric flux of RAC. The RAC that incorporated these materials exhibited reduced electric fluxes relative to the reference sample. At 28 d, the electric fluxes for C-1, C-2, and C-3 were 0.87, 0.79, and 0.73 times that of A-1, respectively. At 90 d, these values further decreased to 0.57, 0.61, and 0.47 times, respectively. The data indicate that the integration of cementitious materials substantially enhances the RAC's resistance to chloride ion penetration, with the combination of FA and GBFS yielding the most pronounced results. This improvement is primarily attributed to the physical adsorption of chloride ions by unhydrated cementitious materials, as well as the chemical reaction between Al_2O_3 present in these materials and chloride ions, which collectively fortify the concrete's resistance to chloride penetration (Shi *et al.* 2017). Additionally, the cementitious materials' filling effect, as previously discussed, contributes to the overall compactness of RAC, further impeding the ingress of chloride ions.

3.4 Pore structure characteristics of RAC

RAC prepared by RA at different heating temperatures were selected for mercury injection test. The mercury injection test results are shown in Table 5. The results in Table 5 show that the porosity of RAC at 120 days of age was 18.124%, 15.347% and 17.335%, respectively. With the increase of heating temperature, the porosity of RAC decreases first and then increases. The reason was that with the increase of temperature, the old mortar attached to the RA was spalling obviously, and the internal structure of the RAC was denser, so the porosity was reduced. If the temperature was too high, the RA would be damaged, and the RA would produce cracks, resulting in an increase in the porosity of the RAC. Therefore, with the increase of temperature, the RAC showed an increase in porosity.

4. Conclusions

Shrinkage and chloride penetration resistance of concrete prepared with RA by heating modified were investigated in this study. The conclusions can be drawn based on the experimental results as following:

- As the replacement percentage of RA increase, the compressive strength and chloride penetration resistance of concrete show a decrease, while the shrinkage values of the mortar increase. Therefore, it is recommended that the replacement percentage of RA should not exceed 50%.
- In the process of heating modified reclaimed coarse aggregate, the heating temperature of 500 ℃ was selected.
- The physical adsorption and chemical reaction of the cementitious material to chloride ions contribute to the mechanical property, shrinkage and chloride penetration resistance of concrete.
- Heating recycled aggregates (RA) to 500 ℃ optimally removes the adhered old mortar through spalling, thereby enhancing the compactness of recycled aggregate concrete (RAC) by reducing interfacial porosity and improving the structural integrity of the cementitious matrix.
- Based on the findings, we recommend limiting the replacement ratio of recycled aggregates (RA) to ≤50% in practical applications, coupled with preheating RA at 500°C to enhance interfacial bonding. Incorporating 20-30% supplementary cementitious materials (SCMs), such as fly ash or slag, is advised to mitigate shrinkage and improve chloride penetration resistance.
- Future research should prioritize hybrid modification techniques (e.g., synergistic heating and carbonation) to further optimize RA quality, alongside long-term field monitoring to validate durability under real-world conditions. Additionally, developing machine learning-driven multiscale performance prediction models will accelerate intelligent material design.

Acknowledgments

The authors acknowledge the financial support of the Prefabricated Building Research Institute of Anhui Province (No. AHZPY2022KF02) and the Science and Technology Research Project of Henan Province(No.252102230050).

References

Bravo, M., Brito, J.D., Pontes, J. and Evangelista, L. (2015), "Durability performance of concrete with recycled aggregates from construction and demolition waste plants", *Constr. Build. Mater.*, **77**, 357-369. https://doi.org/10.1016/j.conbuildmat.2014.12.103.

Butler, L., West, J.S. and Tighe, S.L. (2013), "Effect of recycled concrete coarse aggregate from multiple sources on the hardened properties of concrete with equivalent compressive strength", *Constr. Build. Mater.*, **47**, 1292-1301. https://doi.org/10.1016/j.conbuildmat.2013.05.074.

Corinaldesi, V., Donnini, J., Giosué, C., Mobili, A. and Tittarelli, F. (2020), "Durability assessment of recycled aggregate HVFA concrete", *Appl. Sci.*, **10**(18), 6454. https://doi.org/10.3390/APP10186454.

Dapena, E., Alaejos, P., Lobet, A. and Pérez, D. (2011), "Effect of recycled sand content on characteristics of mortars and concretes", *J. Mater. Civil Eng.*, **23**(4), 414-422. https://doi.org/10.1061/(ASCE)MT.1943-5533.0000183.

Ding, Y., Guo, S., Zhang, X., Zhang, M. and Wu, J. (2021), "Effect of basalt fiber on the freeze-thaw resistance of recycled aggregate concrete, *Comput. Concrete*, **28**(2), 115-127. https://doi.org/10.12989/cac.2021.28.2.115.

Domingo, A., Lázaro, C., Gayarre, F.L., Serrano, M.A. and López-Colina, C. (2009), "Long term deformations by creep and shrinkage in recycled aggregate concrete", *Mater. Struct.*, **43**, 1147-1160. https://doi.org/10.1617/s11527-009-9573-0.

Fiol, F., Revilla-Cuesta, V., Skaf, M., Thomas, C. and Manso, J.M. (2023), "Scaled concrete beams containing maximum levels of coarse recycled aggregate: Structural verifications for precast-concrete building applications", *Struct. Concrete*, **24**(3), 3476-3497. https://doi.org/10.1002/suco.202200963.

Fiol, F., Revilla-Cuesta, V., Thomas, C. and Manso, J.M. (2023), "Self-compacting concrete containing coarse recycled precast-concrete aggregate and its durability in marine-environment-related tests", *Constr. Build. Mater.*, **377**, 131084. https://doi.org/10.1016/j.conbuildmat.2023.131084.

Gholampour, A. and Ozbakkaloglu, T.(2018), "Time-dependent and long-term mechanical properties of concretes incorporating different grades of coarse recycled concrete aggregates", *Eng. Struct.*, **157**, 224-234. https://doi.org/10.1016/j.engstruct.2017.12.015.

Gómez Soberón, J.M.V. (2002), "Shrinkage of concrete with replacement of aggregate with recycled concrete aggregate", *SP-209: ACI Fifth International Conference on Innovations in Design with Emphasis on Seismic, Wind, and Environmental Loading, Quality Control, and Innovations in Materials/ Hot-Weather Concreting*, Cancun, Mexico, December.

Grabiec, A.M., lama, J.K., Zawal, D. and Krupa, D. (2012), "Modification of recycled concrete aggregate by calcium carbonate biodeposition", *Constr. Build. Mater.*, **34**, 145-150. https://doi.org/10.1016/j.conbuildmat.2012.02.027.

Ji, T. (2005), "Preliminary study on the water permeability and microstructure of concrete incorporating nano-SiO_2", *Cement Concrete Res.*, **35**(10), 1943-1947. https://doi.org/10.1016/j.cemconres.2005.07.004.

Jiong, F.L., Ze, P.Y., Ping H.Y. and Jian B.W. (2015), "Mechanical properties of recycled fine glass aggregate concrete under uniaxial loading", *Comput. Concrete*, 16(2), 275-285. https://doi.org/10.12989/cac.2015.16.2.275.

Kapoor, K. and Singh, S.P. (2016), "Durability of self-compacting concrete made with recycled concrete aggregates and mineral admixtures", *Constr. Build. Mater.*, **128**, 67-76. https://doi.org/10.1016/j.conbuildmat.2016.10.026.

Kong, D.Y., Lei, T., Zheng, J.J., Ma, C.C., Jiang, J. and Jiang, J. (2010), "Effect and mechanism of surface-coating pozzalanics materials around aggregate on properties and ITZ microstructure of recycled aggregate concrete", *Constr. Build. Mater.*, **24**(5), 701-708. https://doi.org/10.1016/j.conbuildmat.2009.10.038.

Kou, S., Poon, C. and Agrela, F. (2011), "Comparisons of natural and recycled aggregate concretes prepared with the addition of different mineral admixtures", *Cement Concrete Compos.*, **33**, 788-795. https://doi.org/10.1016/j.cemconcomp.2011.05.009.

Kou, S.C. and Poon, C. (2013), "Long-term mechanical and durability properties of recycled aggregate concrete prepared with the incorporation of fly ash", *Cement Concrete Compos.*, **37**, 12-19. https://doi.org/10.1016/j.cemconcomp.2012.12.011.

Ledesma, E.F., Jimenez, J., Ayuso, J. and Godino, F.I. (2016), "Propuesta de máximo uso de arena reciclada de hormigón en el diseo de morteros de albailería", *Mater. Constr.*, **66**(321), e075. https://doi.org/10.3989/mc.2016.08414.

Lotfi, S., Eggimann, M., Wagner, E., Mróz, R. and Deja, J. (2015), "Performance of recycled aggregate concrete based on a new concrete recycling technology", *Constr. Build. Mater.*, **95**, 243-256. https://doi.org/10.1016/j.conbuildmat.2015.07.021.

Marthong, C., Pyrbot, R.N., Tron, S.L., Mawroh, L.I.D., Choudhury, M.S.A. and Bharti, G.S. (2018), "Micro-concrete composites for strengthening of RC frame made of recycled aggregate concrete", *Comput. Concrete*, **22**(5), 461-468. https://doi.org/10.12989/cac.2018.22.5.461.

Mohamed, A.Y., Canpolat, O. and Al-Mashhadani, M.M. (2022), "Mechanical and durability of geopolymer concrete containing fibers and recycled aggregate", *Comput. Concrete*, **30**(6), 421-432. https://doi.org/10.12989/cac.2022.30.6.421.

Mukharjee, B.B. and Barai, S.V. (2014), "Influence of incorporation of nano-silica and recycled aggregates on compressive strength and microstructure of concrete", *Constr. Build. Mater.*, **71**, 570-578. https://doi.org/10.1016/j.conbuildmat.2014.08.040.

Nematzadeh, M. and Baradaran-Nasiri, A. (2019), "Mechanical performance of fiber-reinforced recycled refractory brick concrete exposed to elevated temperatures", *Comput. Concrete*, **24**,19-35. https://doi.org/10.12989/cac.2019.24.1.019.

Pedro, D., de Brito, J. and Evangelista, L. (2014), "Influence of the use of recycled concrete aggregates from different sources on structural concrete", *Constr. Build. Mater.*, **71**, 141-151. https://doi.org/10.1016/j.conbuildmat.2014.08.030.

Pedro, D., de Brito, J. and Evangelista, L. (2017), "Evaluation of high-performance concrete with recycled aggregates: Use of densified silica fume as cement replacement", *Constr. Build. Mater.*, **147**, 803-814. https://doi.org/10.1016/j.conbuildmat.2017.05.007.

Pelisser, F., Zavarise, N., Longo, T.A. and Bernardin, A.M. (2011), "Concrete made with recycled tire rubber: Effect of alkaline activation and silica fume addition", *J. Clean. Prod.*, **19**, 757-763. https://doi.org/10.1016/j.jclepro.2010.11.014.

Rajhans, P., Gupta, P.K., Ranjan, R.K., Panda, S.K. and Nayak, S. (2018), "EMV mix design method for preparing sustainable self compacting recycled aggregate concrete subjected to chloride environment", *Constr. Build. Mater.*, **199**, 705-716. https://doi.org/10.1016/j.conbuildmat.2018.12.079.

Rajhans, P., Panda, S.K. and Nayak, S. (2018), "Sustainability on durability of self compacting concrete from C&D waste by improving porosity and hydrated compounds: A microstructural investigation", *Constr. Build. Mater.*, **174**, 559-575. https://doi.org/10.1016/j.conbuildmat.2018.04.137.

Sainz-Aja, J.A., Carrascal, I.A., Polanco, J.A. and Thomas, C. (2022), "Effect of temperature on fatigue behaviour of self-compacting recycled aggregate concrete", *Cement Concrete Compos.*, **125**, 104309. https://doi.org/10.1016/j.cemconcomp.2021.104309.

Santamaría, A., Revilla-Cuesta, V., Skaf, M. and Romera, J.M. (2023), "Full-scale sustainable structural concrete containing high proportions of by-products and waste", *Case Stud. Constr.*

Mater., **18**, e02142. https://doi.org/10.1016/j.cscm.2023.e02142.
Sasanipour, H. and Aslani. F. (2019), "Durability properties evaluation of self-compacting concrete prepared with waste fine and coarse recycled concrete aggregates", *Constr. Build. Mater.*, **236**, 117540. https://doi.org/10.1016/j.conbuildmat.2019.117540.
Seara-Paz, S., Corinaldesi, V., González-Fonteboa, B. and Martínez-Abella, F. (2016), "Influence of recycled coarse aggregates characteristics on mechanical properties of structural concrete", *Eur. J. Environ. Civil Eng.*, **20**(sup1), s123-s139. https://doi.org/10.1080/19648189.2016.1246694.
Seara-Paz, S., González-Fonteboa, B. and Martínez-Abella, F.I. (2016), "Creep and shrinkage", *Constr. Build. Mater.*, **122**, 95-109. https://doi.org/10.1016/j.conbuildmat.2016.06.050.
Seara-Paz, S., González-Fonteboa, B., Martínez-Abella, F. and Eiras-López, J. (2018), "Flexural performance of reinforced concrete beams made with recycled concrete coarse aggregate", *Eng. Struct.*, **156**, 32-45. https://doi.org/10.1016/j.engstruct.2017.11.015.
Shi, C.J., Hu, X., Wang, X.G., Wu，Z. and Schutter, G.D. (2017), "Effects of chloride ion binding on microstructure of cement pastes", *J. Mater. Civil Eng.*, **29**(1), 04016183.
Shi, C.J., Li, Y.K., Zhang, J.K., Li, W.G., Chong, L.L. and Xie, Z.B. (2016), "Performance enhancement of recycled concrete aggregate - A review", *J. Clean. Prod.*, **112**(1), 446-472. https://doi.org/10.1016/j.jclepro.2015.08.057.
Su, Y., Gu, S., Chang, X.L. and Li, J.X. (2015), "Experimental study on heating modified recycled concrete coarse aggregate", *China Concrete Cement Prod.*, **2015**(10), 6-10. https://doi.org/10.19761/j.1000-4637.2015.10.002.
Tahmouresi, B., Koushkbaghi, M., Monazami, M., Abbasi, M.T. and Nemati, P. (2019), "Experimental and statistical analysis of hybrid-fiber-reinforced recycled aggregate concrete", *Comput. Concrete*, **24**(3), 193-206. https://doi.org/10.12989/cac.2019.24.3.193.
Tung, T.M., Le, D.H. and Babalola, O.E. (2023), "Prediction of residual compressive strength of fly ash based concrete exposed to high temperature using GEP", *Comput. Concrete*, **31**(2), 111-121. https://doi.org/10.12989/cac.2023.31.2.111.
Wang, L., Wang, J., Qian, X., Chen, P., Xu, Y. and Guo, J. (2017), "An environmentally friendly method to improve the quality of recycled concrete aggregates", *Constr. Build. Mater.*, **144**, 432-441. https://doi.org/10.1016/j.conbuildmat.2017.03.191.
Xiang, G.Z., Gao, Q.Z., Xu, Y.L., Yu, H.F., Ercong, M., Jun, M.Y. and Ya, J.H. (2023), "Experimental and numerical analysis of seismic behaviour for recycled aggregate concrete filled circular steel tube frames", *Comput. Concrete*, **31**(6), 537-543. https://doi.org/10.12989/cac.2023.31.6.537.
Xiao, J., Li, L., Shen, L. and Poon, C.S. (2015), "Compressive behaviour of recycled aggregate concrete under impact loading", *Cement Concrete Res.*, **71**, 46-55. https://doi.org/10.1016/j.cemconres.2015.01.014.
Xie, J.H., Guo, Y.C., Liu, L.S. and Xie, Z.H. (2015), "Compressive and flexural behaviours of a new steel-fibre-reinforced recycled aggregate concrete with crumb rubber", *Constr. Build. Mater.*, **15**, 263-272. https://doi.org/10.1016/j.conbuildmat.2015.01.036.
Zega, C.J., Coelho Dos Santos, G.S., Villagrán-Zaccardi, Y.A. and Di Maio, A.A. (2016), "Performance of recycled concretes exposed to sulphate soil for 10 years", *Constr. Build. Mater.*, **102**, 714-721. https://doi.org/10.1016/j.conbuildmat.2015.11.025.
Zhang, H. and Zhao, Y. (2015), "Integrated interface parameters of recycled aggregate concrete", *Constr. Build. Mater.*, **101**, 861-877. https://doi.org/10.1016/j.conbuildmat.2015.10.084.
Zhang, H., Wang, Y.Y., Lehman, D.E. and Geng, Y. (2020), "Autogenous-shrinkage model for concrete with coarse and fine recycled aggregate", *Cement Concrete Compos.*, **111**, 103600. https://doi.org/10.1016/j.cemconcomp.2020.103600.
Zhu, X., Chen, X., Shen, N., Tian, H., Fan, X. and Lu, J. (2018), "Mechanical properties of pervious concrete with recycled aggregate", *Comput. Concrete*, **21**(6), 623-635. https://doi.org/10.12989/cac.2018.21.6.623.

CC